Experimental Evidence of Phospho*enol*pyruvate Resynthesis from Pyruvate in Illuminated Leaves[1][W]

Guillaume Tcherkez*, Aline Mahé, Edouard Boex-Fontvieille, Elisabeth Gout, Florence Guérard, and Richard Bligny

Institut de Biologie des Plantes, Centre National de la Recherche Scientifique Unité Mixte de Recherche 8618 (G.T., A.M., E.B.-F.), and Plateforme Métabolisme-Métabolome, Institut Fédératif de Recherche 87 (G.T., F.G.), Université Paris-Sud, 91405 Orsay cedex, France; Institut Universitaire de France, 75005 Paris, France (G.T.); and Laboratoire de Physiologie Cellulaire Végétale, Unité Mixte de Recherche 5168, Commissariat à l'Energie Atomique Grenoble, 38054 Grenoble cedex 9, France (E.G., R.B.)

Day respiration is the cornerstone of nitrogen assimilation since it provides carbon skeletons to primary metabolism for glutamate (Glu) and glutamine synthesis. However, recent studies have suggested that the tricarboxylic acid pathway is rate limiting and mitochondrial pyruvate dehydrogenation is partly inhibited in the light. Pyruvate may serve as a carbon source for amino acid (e.g. alanine) or fatty acid synthesis, but pyruvate metabolism is not well documented, and neither is the possible resynthesis of phospho*enol*pyruvate (PEP). Here, we examined the capacity of pyruvate to convert back to PEP using ^{13}C and ^{2}H labeling in illuminated cocklebur (*Xanthium strumarium*) leaves. We show that the intramolecular labeling pattern in Glu, 2-oxoglutarate, and malate after ^{13}C-3-pyruvate feeding was consistent with ^{13}C redistribution from PEP via the PEP-carboxylase reaction. Furthermore, the deuterium loss in Glu after $^{2}H_3$-^{13}C-3-pyruvate feeding suggests that conversion to PEP and back to pyruvate washed out ^{2}H atoms to the solvent. Our results demonstrate that in cocklebur leaves, PEP resynthesis occurred as a flux from pyruvate, approximately 0.5‰ of the net CO_2 assimilation rate. This is likely to involve pyruvate inorganic phosphate dikinase and the fundamental importance of this flux for PEP and inorganic phosphate homeostasis is discussed.

It has now been 63 years since Kok described the effect by which nonphotorespiratory CO_2 evolution increases at low light levels, providing evidence for the inhibition of leaf respiration by light (Kok, 1948). Since then, respiration of illuminated leaves (day respiration) and its inhibition has been extensively characterized with gas-exchange and metabolic analyses (for review, see Atkin et al., 2000). Recent articles have further emphasized the complex metabolic relationships between day respiration and other metabolic processes such as nitrogen metabolism, since carbon (C) skeletons synthesized by the tricarboxylic acid pathway (TCAP) are essential for nitrogen assimilation (Paul and Pellny, 2003; Nunes-Nesi et al., 2007). The metabolic mechanisms by which respiratory metabolism is down-regulated in the light has been summarized previously (Tcherkez et al., 2009). Essentially, the activity of the TCAP has been shown to be strongly inhibited (Hanning and Heldt, 1993; Tcherkez et al., 2005; Gauthier et al., 2010); therefore, the consumption of pyruvate molecules synthesized in the light by the TCAP is believed to be limited.

This raises the question of the fate of pyruvate and acetyl-CoA produced by the pyruvate dehydrogenase (PDH; Fig. 1, arrow 1). Acetyl-CoA is not likely to accumulate. First, the PDH is retroinhibited by its product acetyl-CoA (Harding et al., 1970; Rapp et al., 1987), and PDH activity is down-regulated by phosphorylation (Budde and Randall, 1990; Tovar-Méndez et al., 2003). This effect may in turn contribute to the buildup of the pyruvate pool. Second, a significant fraction of acetyl-CoA is directed to fatty acids production in the chloroplast (Ohlrogge and Jaworski, 1997). Accordingly, the antisense line of Arabidopsis (*Arabidopsis thaliana*) associated with PDH kinase (in which the mitochondrial PDH reaction is thus enhanced) accumulated ^{14}C-labeled fatty acids when ^{14}C-Pyr was fed to photosynthetic stems (Marillia et al., 2003).

By contrast, pyruvate is believed to accumulate to some extent in the light. Metabolic measurements in leaves along a day/night cycle have shown that the pyruvate content is roughly 2-fold larger in the light (Scheible et al., 2000). Pyruvate is also converted to Ala, as shown by ^{13}C labeling (Tcherkez et al., 2005; Fig. 1, arrow 2). That said, pyruvate production itself (by pyruvate kinase, EC 2.7.1.40; Fig. 1, arrow 3) is

[1] This work was supported by the Agence Nationale de la Recherche, with the project Jeunes Chercheurs (grant no. JC08–330055 to G.T., A.M., and E.B.-F.).

* Corresponding author; e-mail guillaume.tcherkez@u-psud.fr.

The author responsible for distribution of materials integral to the findings presented in this article in accordance with the policy described in the Instructions for Authors (www.plantphysiol.org) is: Guillaume Tcherkez (guillaume.tcherkez@u-psud.fr).

[W] The online version of this article contains Web-only data.

www.plantphysiol.org/cgi/doi/10.1104/pp.111.180711

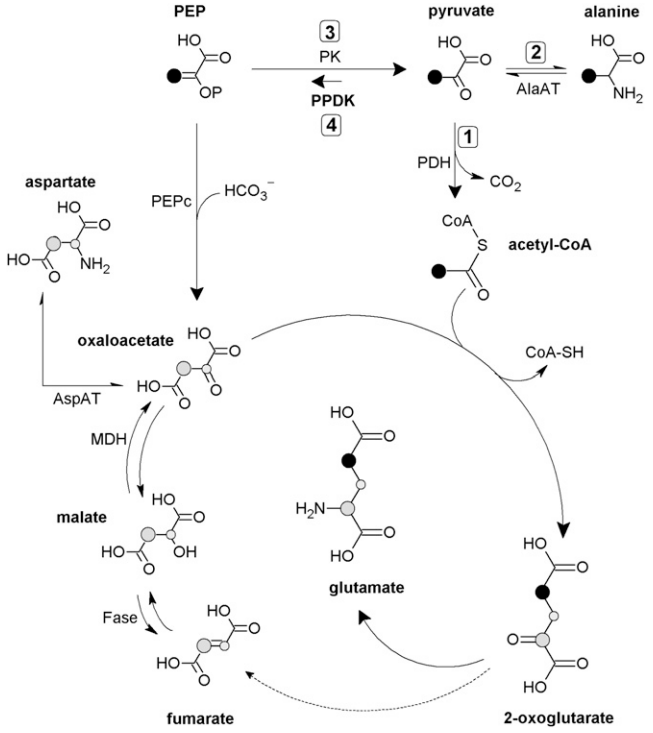

Figure 1. Simplified metabolic scheme showing the potential fates of pyruvate and the labeling pattern after ^{13}C-3-pyruvate addition to illuminated leaves. The labeled position in C-3-pyruvate and molecules downstream through PDH (1), AlaAT (2), and the tricaboxylic acid cycle is shown in black. Labeled C-atom positions coming from PPDK (4) or reverse pyruvate kinase (PK, 3) activity are shown in gray. The small gray-labeled C atom accounts for the fumarate/malate equilibrium that interconverts C-2 and C-3 atoms due to molecular symmetry. This scheme does not take into account multiple turns of the tricarboxylic acid cycle and assumes little conversion of 2-oxoglutarate to fumarate (dashed arrow, see main text and Tcherkez et al., 2009). AspAT, Asp aminotransferase; Fase, fumarase; MDH, malate dehydrogenase.

believed to be partly inhibited in the light, due to the regulatory properties of the enzyme. In tobacco (*Nicotiana tabacum*) leaves, the total activity of pyruvate kinase has been shown to be lower in the light compared to the dark (Scheible et al., 2000), and in spinach (*Spinacia oleracea*) chloroplasts, the pyruvate content appeared lower in the light than in the dark (Santarius and Heber, 1965). In the alga *Selenastrum minutum*, the chloroplastic enzyme is inhibited by photosynthetic intermediates (e.g. ribulose-1,5-bisphosphate) and the cytosolic enzyme is inhibited by inorganic phosphate (Pi) and Glu (Lin et al., 1989). Furthermore, leaf enzymes are inhibited by citrate or Asp (Baysdorfer and Bassham, 1984) and activated by dihydroxyacetone phosphate (Lin et al., 1989). Therefore in the light, pyruvate kinase activity is presumed to be strongly down-regulated in chloroplasts and finely adjusted (by the balance between upstream and downstream metabolites) in the cytosol.

Still, the reverse reaction, that is, resynthesis of phospho*enol*pyruvate (PEP) from pyruvate (Fig. 1, arrow 4), is not well documented. In principle, the pyruvate kinase is reversible (Krimsky, 1959; Robinson and Rose, 1972; Dyson et al., 1975), but under ordinary conditions, the reaction has a large equilibrium constant toward pyruvate production (Krimsky, 1959; McQuate and Utter, 1959; Nageswara-Rao et al., 1979; Supplemental Table S1). The reverse reaction, if it happens to occur, may be assumed to rather involve the pyruvate Pi dikinase (PPDK; EC 2.7.9.1). This enzyme has recently been found and characterized in Arabidopsis leaves, in which there are two isoforms (cytosolic and chloroplastic; for review, see Chastain and Chollet, 2003). Furthermore, a light/dark regulation of the leaf enzyme involving phosphorylation has been demonstrated (Chastain et al., 2002). However, the function of the enzyme remains enigmatic. Some data suggest a role in the response to stress such as anoxia (Lasanthi-Kudahettige et al., 2007; Doubnerová and Ryšlavá, 2011). In seeds, PPDK activity seems essential in controlling starch biosynthesis by providing cytosolic pyrophosphate (PPi) and hexose phosphates via reversed glycolysis (Kang et al., 2005). In leaves, substantial midvein PPDK activity has been demonstrated, suggesting a role in providing PEP to the shikimate pathway for lignin biosynthesis (Hibberd and Quick, 2002). Transcripts encoding cytosolic PPDK have been shown to increase during senescence of Arabidopsis leaves (Lin and Wu, 2004; Taylor et al., 2010) so that PPDK activity has been assumed to participate in nitrogen remobilization associated with leaf senescence (Taylor et al., 2010): PEP synthesized from pyruvate by PPDK is believed to be converted to organic acids via PEP-carboxylase (PEPc), thus sustaining the production of the transport amino acid Gln.

Here, we examined the metabolic flux associated with the possible conversion of pyruvate back to PEP in illuminated leaves, using strong isotopic labeling with protio-^{13}C- and deutero-^{13}C-pyruvate ($^{2}H_3$-^{13}C-3-pyruvate, thereafter denoted as *d*-^{13}C-3-pyruvate). The fate of ^{13}C atoms was then followed by NMR. We took advantage of the contrasted enrichment pattern expected when conversion back to PEP is involved (Fig. 1): PEP resynthesis followed by PEP carboxylation mostly redistributes the ^{13}C label in the C-2 atom position of Glu, whereas the ^{13}C-3-pyruvate consumption by the TCAP produces ^{13}C-4-Glu. We show that pyruvate can be converted back to PEP, although the associated flux is quantitatively minor. Our data thus suggest that PEP resynthesis contributes to consuming pyruvate molecules that tend to accumulate in the light.

RESULTS

^{13}C-Labeling Pattern in Metabolites

The ^{13}C-labeling pattern in major metabolites after $^{13}CO_2$ and/or ^{13}C-3-pyruvate feeding is shown in

Figure 2. As expected, ^{13}C-pyruvate labeling caused an isotopic enrichment (positional percentage ^{13}C) up to 15% in Glu C-4 and Gln C-4, and 6% in isocitrate C-4, reflecting the consumption of the ^{13}C label by the TCAP. There is also a clear ^{13}C enrichment in malate C-3 (15%) and Glu C-3 (3.5%; and also Glu C-2, see the next section), suggesting either the involvement of the production of malate from PEP resynthesized from ^{13}C-3-pyruvate, or several rounds of the TCAP cycle (Fig. 1). However, succinate and fumarate were not labeled, strongly suggesting that most ^{13}C atoms were not committed into the full cycle, that is, multiple rounds cannot account for the neat labeling in malate C-3. ^{13}C-3-pyruvate was also consumed by amino acid synthesis, such as Ala (3% ^{13}C in C-3) and Val (34% ^{13}C in methyl groups). The labeling was accompanied by a small refixation of $^{13}CO_2$ produced by the decarboxylation of ^{13}C-3-pyruvate (by the TCA cycle). Such a refixation was very small, with 5% ^{13}C in furano-Fru C-2 and 3% ^{13}C in both α-Glc and the glucosyl moiety of Suc. Using metabolite contents, this demonstrates that ^{13}C refixation was, at most, of 6% of the TCAP ^{13}C commitment to Glu.

When leaves were labeled with $^{13}CO_2$, most sugars showed a clear ^{13}C enrichment, as well as malate and Asp C-2, showing the involvement of the PEPc reaction from ^{13}C-2-enriched PEP that was in turn formed by glycolysis. When both ^{13}C-3-pyruvate and $^{13}CO_2$ were used, the effect of the double labeling was not simply additive. In fact, the C-1 in malate was clearly labeled (9% ^{13}C), suggesting ^{13}C-bicarbonate fixation by the PEPc in C-4 and subsequent equilibration to C-1 via fumarate; similarly, C-1, C-2, and C-3 positions in Glu were labeled (up to 11%), indicating the consumption of malate formed from ^{13}C-enriched PEP.

Specific ^{13}C Pattern in Glu

The specific ^{13}C-enrichment pattern in Glu is detailed in Figure 3. The positional ^{13}C abundance found in Glu C-1 upon ^{13}C-3-pyruvate labeling was 1.7%, very close to the natural abundance (1.1%, dashed line in Fig. 3B). The ^{13}C abundance in C-2 and C-3 was 3% to 4%, showing the redistribution of the ^{13}C label. The percentage ^{13}C in C-4 was very high because it inherited the ^{13}C label via the TCAP (Fig. 1). With $^{13}CO_2$, the reverse occurred, the C-4 position being at natural abundance, whereas the C-1 to C-3 positions were labeled 3% to 4% ^{13}C.

The positional labeling in Glu was associated with {^{13}C-^{13}C} interactions between neighbor C atoms (Fig. 3C). Upon ^{13}C-3-pyruvate labeling, the most labeled position (C-4) was associated with little interaction (6% only of ^{13}C-4 atoms were accompanied by a ^{13}C neighbor), whereas the interaction was 62% in C-3. In other words, most ^{13}C-3-Glu molecules were also labeled on a neighbor C, whereas most ^{13}C-4-Glu molecules were not labeled on a neighbor C. This indicates that presumably, the consumption of ^{13}C-2-oxaloacetate molecules by the TCAP mostly used ^{13}C-2-acetyl-CoA, whereas the reciprocal was not true (most ^{13}C-2-acetyl-CoA molecules did not react with ^{13}C-2-oxaloacetate). The C-2 atom position in Glu did not show visible {^{13}C-^{13}C} interaction.

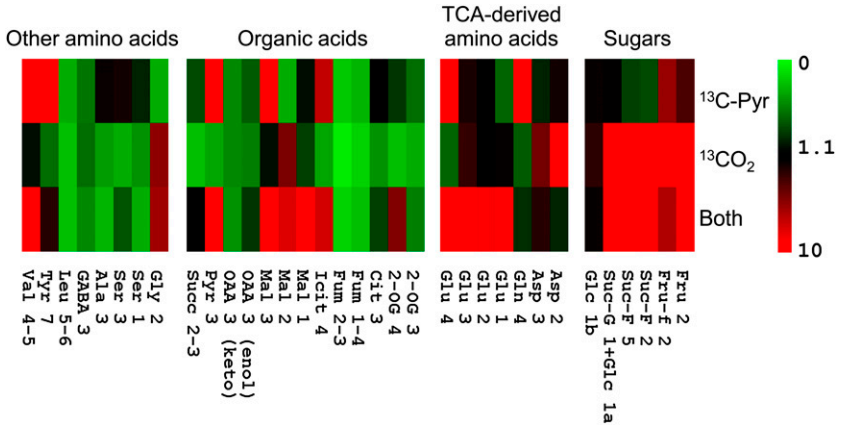

Figure 2. Labeling patterns in visible C-atom positions in metabolites, detected with ^{13}C-NMR after ^{13}C-3-pyruvate and/or $^{13}CO_2$ labeling of illuminated cocklebur leaves for 3 h, under 400 μmol mol^{-1} CO_2, 21% O_2, 23.5°C, and 300 μmol m^{-2} s^{-1} PAR. In each cell, the color represents the positional ^{13}C abundance in percent (%) ^{13}C (color scale on the right). C-atom positions are numbered according to the international chemical nomenclature (for Glu, see Fig. 3). For Glc, a and b stand for alpha and beta isomers. For the C-3 atom position in oxalo acetate, the two isomeric forms are distinguished: C=O (keto) and C-OH (enol). The average abundance chosen here (1.1%) corresponds to the natural ^{13}C abundance. ^{13}C-abundance values shown here are means of three replicates. The color scale is here restricted to 10% so as to make low ^{13}C enrichments visible. Fumarate never appears labeled due to isotopic dilution caused by its very large content in cocklebur leaves (near 20 mmol m^{-2}, not shown here). The C-5 atom position in Glu and C-4 atom position in malate are not shown here because of insufficient signal intensity or resolution. Cit, Citrate; Fru, Fru (pyranic form); Fru-f, Fru (furanic form); Fum, fumarate; GABA, γ-aminobutyrate; Glc 1b, 1a, C-1 position of alpha and beta enantiomers of Glc; Icit, isocitrate; Mal, malate; 2-OG, 2-oxoglutarate; OAA, oxalo acetate; Pyr, pyruvate; Suc-G, glucosyl moiety of Suc; Suc-F, Fru moiety of Suc; Succ, succinate.

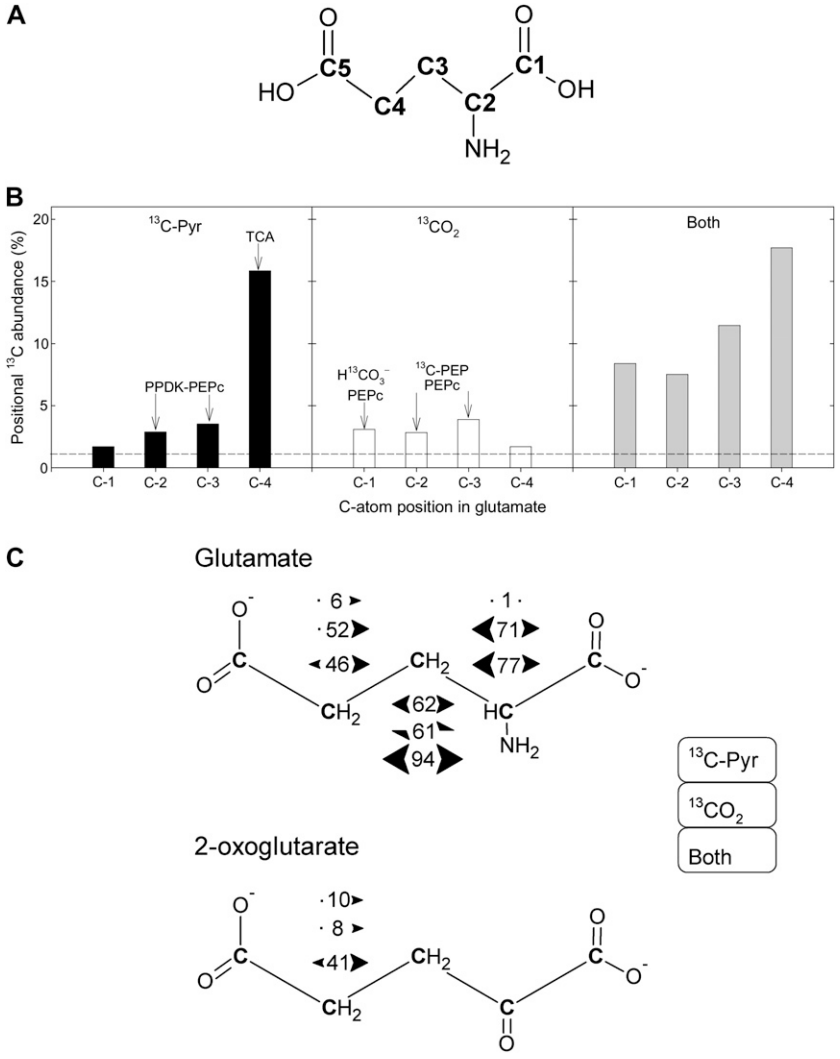

Figure 3. Positional ^{13}C-NMR signals in Glu, after ^{13}C-3-pyruvate and/or $^{13}CO_2$ labeling of illuminated cocklebur leaves for 3 h, under 400 μmol mol^{-1} CO_2, 21% O_2, 23.5°C, and 300 μmol m^{-2} s^{-1} PAR. A, C-atom numbering in Glu. B, Positional ^{13}C abundance (in % ^{13}C) in Glu (redrawn from Fig. 2). The natural ^{13}C abundance (1.1%) is indicated with the horizontal dashed line. The major origin of ^{13}C labeling in each position is indicated with arrows, as discussed in the main text. C, {^{13}C-^{13}C} spin-spin interactions in Glu. For a given labeled position, numbers between arrows indicate the percentage of C atoms having ^{13}C labeling in the neighbor C atoms. Bidirectional arrows indicate that two {^{13}C-^{13}C} interactions were obtained, demonstrating there were two interacting, labeled neighbor C. For example, in C-3 Glu after pyruvate labeling, the percentage of ^{13}C in C-3 that was accompanied by ^{13}C in C-2 and C-4 was 62%. In 2-oxoglutarate, {^{13}C-^{13}C} spin-spin interactions were only visible (distinguishable from the background) in C-4 because of the larger ^{13}C enrichment in that position. The value of 1% (Glu C-2 upon ^{13}C-pyruvate labeling) is arbitrary and corresponds to the natural interaction (^{13}C natural abundance of 1.1%). Bidirectional half arrows indicate that a single {^{13}C-^{13}C} interaction occurred, on one side only of the C-atom position considered. From top to bottom, interactions values indicated here are that observed after ^{13}C-pyruvate labeling, $^{13}CO_2$ labeling, and after double labeling, in that order.

Upon $^{13}CO_2$ labeling, there were substantial {^{13}C-^{13}C} interactions, with the largest value in C-2, suggesting that ^{13}C-2-oxaloacetate molecules were clearly coupled to the input of ^{13}C-2-acetyl-CoA. Similarly, double labeling with $^{13}CO_2$ and ^{13}C-3-pyruvate lead to nearly 100% {^{13}C-^{13}C} interaction in C-3 with a clear double interaction (on both C-2 and C-4 sides), showing the concerted contribution of ^{13}C-2-oxaloacetate and ^{13}C-2-acetyl-CoA to produce Glu. Furthermore, the largest interaction values were obtained with C-2 and C-3 positions (77% and 94% versus 46% in C-4), suggesting the involvement of $^{13}C_2$-2,3-oxaloacetate (Fig. 1). In 2-oxoglutarate, significant {^{13}C-^{13}C} interaction was only visible in C-4 (see also Supplemental Fig. S1), with a larger value upon double labeling that was consistent with that found in Glu C-4. The C-2 position in 2-oxoglutarate corresponds to the C=O (keto) C atom and was therefore difficult to analyze by NMR because of long relaxation time, about 30 s (remote chemical shift region), that caused an underestimation of corresponding resonance peaks. That said, there appeared to be no substantial labeling in that position (Supplemental Fig. S1).

Proton Exchange in Glu C-4

^{13}C labeling was carried out with either protonated (CH_3-CO-COO^-) or deuterated (50% CD_3-CO-COO^-) pyruvate. The labeling pattern in metabolites upon *d*-^{13}C-3-pyruvate was very similar to that in Figure 2 (not shown). The resolution and intensity of deuterated ^{13}C-pyruvate were not large enough to appreciate deuterium content directly on the pyruvate pool. Therefore, the fate of deuterium was followed using the {^{13}C-D} interaction on Glu C-4. The NMR signal obtained is shown in Figure 4. Clearly, a significant fraction of ^{13}C-4-Glu molecules were also deuterated, causing a change of around 0.25 ppm (28 Hz) on the ^{13}C chemical shift, with the appearance of a triplet. Deuterated Glu was found to represent 33% of total ^{13}C-4-Glu. That value is significantly less than that in source pyruvate (50%), suggesting a loss of deuterium

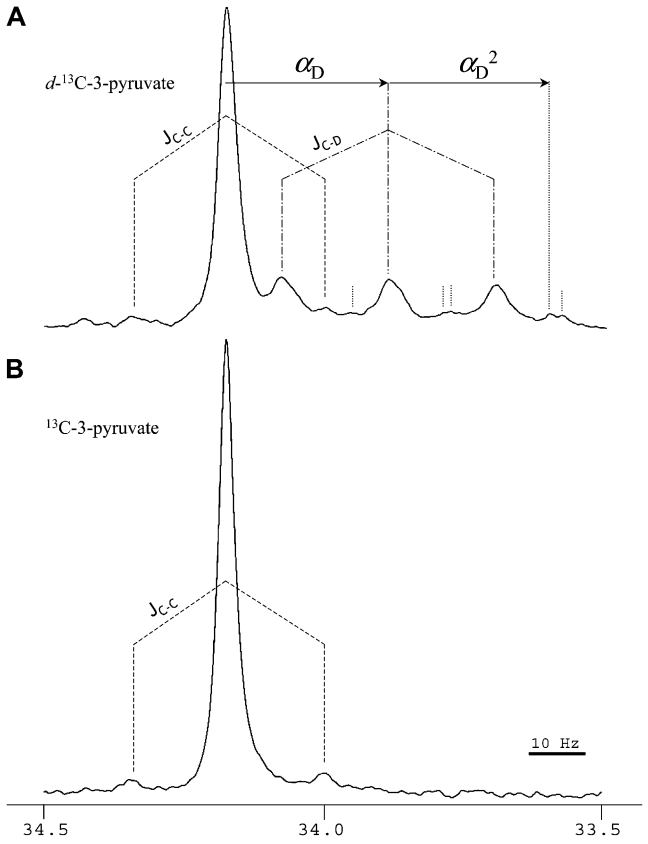

Figure 4. The 33.5 to 34.5 ppm region of the NMR spectrum showing the ^{13} signal of the C-4 atom position in Glu in illuminated cocklebur leaves after deutero-^{13}C-3-pyruvate (A) or protio-^{13}C-3-pyruvate (B) labeling for 3 h, under 400 μmol mol^{-1} $^{12}CO_2$, 21% O_2, 23.5°C, and 300 μmol m^{-2} s^{-1} PAR. {^{13}C-^{13}C} and {^{13}C-D} single interactions are shown with dashed (J_{C-C}) and dash-dotted lines (J_{C-D}), respectively. In A, the deuterium isotope effect on the chemical shift is indicated with the arrow labeled α_D (single deuteration, CHD) and α_D^2 (double deuteration, CD_2). Peaks associated with the double deuteration are labeled with dotted vertical lines (other peaks beyond 33.5 ppm are not shown here). The area integration indicates that the proportion of deuterated ^{13}C atoms is 33% and the ^{13}C-interacting ^{13}C atoms is 5.0% of ^{13}C atoms. In B, the interaction with neighbor ^{13}C atoms represents 4.5%.

during metabolism of pyruvate to Glu. This effect may have come from either the hydrogen/deuterium isotope effect of citrate synthase (the other two first enzymes of the TCA cycle, aconitase and isocitrate dehydrogenase, do not involve the CH_2 protons along their mechanism) or the wash out of deuterium atoms to the solvent due to pyruvate enolization. However, we found no significant isotope effect on the ^{13}C amount in Glu (37 and 41 μmol m^{-2} [internal standard equivalents] with deutero- and protio-^{13}C-3-pyruvate, respectively), showing that the rate of ^{13}C-3-pyruvate incorporation by citrate synthase was not slowed down by deuterium under our conditions. The loss of deuterium was thus caused by isotopic wash out associated with pyruvate conversion to PEP.

PPDK Activity and Phosphometabolites

Total leaf PPDK activity was measured from illuminated leaves and also during the night (1 h 30 dark; Fig. 5C). The activity was clearly lower in the dark than in the light. Still, the in vitro activity value found here (0.04 μmol m^{-2} s^{-1}) in the light was very small as compared to photosynthesis (near 10 μmol m^{-2} s^{-1}, data not shown). There was a significant decrease (2-fold) of the pyruvate content in the dark, whereas the PEP content decreased a bit less, from 2.9 to 1.7 μmol m^{-2} (Fig. 5A). Leaf ATP-ADP ratio decreased from around 2.5 in the light to 1.2 in the dark and the ATP-AMP ratio remained unchanged (around 3; Fig. 5B). Therefore, the mass action ratio of pyruvate kinase ([pyruvate/PEP] $\times$ [ATP/ADP]) appeared to be less favorable to the reaction in the light than in the dark. The corresponding mass action ratio of PPDK ([PEP/pyruvate] $\times$ [AMP/ATP]) was less favorable to the reaction in the dark, provided PPi remained constant (not measured here, not visible on NMR analyses).

The natural covariation in phosphometabolites was investigated, using six replicates of leaves sampled in identical photosynthetic conditions, with pyruvate feeding (Fig. 6). Hierarchical clustering analysis shows that PEP was in the same group as AMP, ADP, Fru-1,6-bisphosphate, ribulose-1,5-bisphosphate, ATP, and ADP-Glc (group II, Fig. 6C), that is, primary photosynthetic phosphometabolites. That is, net PEP production covaried tightly with chloroplastic photosynthetic activity (rather than cytosolic metabolites such as UDP-Glc). PEP-AMP and PEP-Fru-1,6-bisphosphate ratios were rather constant (Fig. 6B), for any UDP-Glc/UTP values. Furthermore, when plotted against Fru-1,6-bisphosphate, [PEP $\times$ AMP]/[ATP] increased and so did the [PEP $\times$ ADP]/[ATP] ratio. In other words, there was a positive relationship between the mass action ratio of pyruvate kinase and the phosphohexose content.

DISCUSSION

The metabolism of pyruvate in illuminated C_3 leaves is not very well documented and much uncertainty remains on metabolic fluxes associated with the different pathways that consume pyruvate. Here, we used isotopic labeling to investigate whether the resynthesis of PEP from pyruvate occurred in the light, by the involvement of, e.g. PPDK. First, we carried out labeling with ^{13}C-3-pyruvate to trace the possible redistribution of ^{13}C in C-atom positions derived from PEP C-3 (Fig. 1). Second, we used deuterated ^{13}C-3-pyruvate (double labeling) to examine whether deuterium atoms were preserved in ^{13}C-4-Glu. Third, we measured leaf PPDK activity and phosphometabolites so as to better understand PEP metabolism.

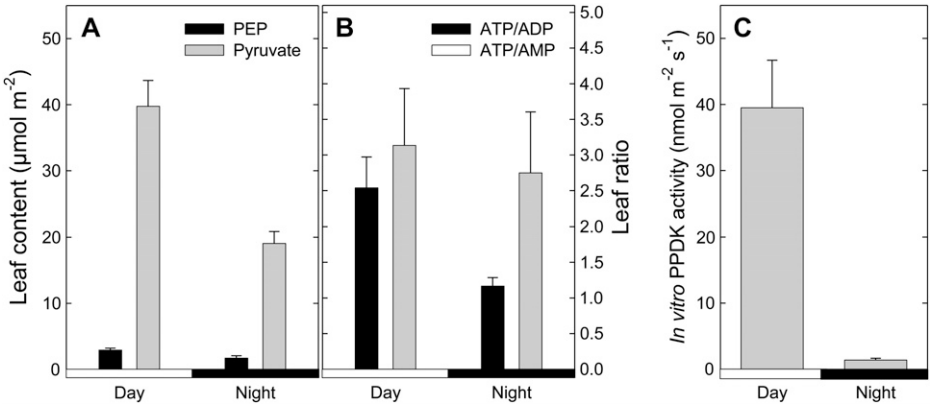

Figure 5. Leaf metabolic amounts (A and B) and PPDK activity (C) in cocklebur, in the dark and in the light (400 μmol mol^{-1} CO_2, 21% O_2, 23.5°C, 300 μmol mol^{-1} PAR, no labeling). PEP content was determined by quantitative ^{31}P-NMR from perchloric extracts. ATP-ADP and ATP-AMP ratios were measured on the same extracts with liquid-chromatography/time-of-flight mass spectrometry. In vitro PPDK activity (nmol PEP m^{-2} s^{-1}) was measured on desalted leaf extracts using a PEPc-malate dehydrogenase coupled enzymatic assay. Values are mean ± SE (n = 3).

Is Pyruvate Converted Back to PEP?

After ^{13}C-3-pyruvate labeling, we found a clear labeling in C-atom positions (Glu C-4, Gln C-4, isocitrate C-4) inherited from the TCAP activity that consumes ^{13}C-2-acetyl-CoA formed from pyruvate. Such results are consistent with those obtained in cocklebur (*Xanthium strumarium*) in similar conditions (Tcherkez et al., 2008, 2009) and show that Glu was one major sink metabolite after pyruvate addition (nearly 30% of total nonsugar ^{13}C in samples). Importantly, ^{13}C atoms were also redistributed in positions inherited from PEP, such as malate C-3. Furthermore, although not very visible, oxaloacetate showed a very slight increase from 1.4% to 2% ^{13}C in C-3 (Fig. 2).

It remains possible that ^{13}C-3-pyruvate caused a labeling in malate and oxaloacetate via several rounds of the TCAP (Krebs cycle). However, under such an assumption, the isotopic pattern in malate would show a larger enrichment in C-2 than in C-3. Here, malate C-2 is not labeled (Fig. 2). In addition, previous studies in cocklebur showed the accumulation of fumarate and Glu, with no possible ^{13}C labeling in succinate, thereby showing the noncyclic nature of the TCAP (Tcherkez et al., 2009) with a 5% to 10% recovery of 2-oxoglutarate back to citrate through the cycle. Furthermore, the isotopic pattern found in Glu was not strictly consistent with a cycle-based ^{13}C redistribution. We show that the probability to observe a neighbor ^{13}C associated with Glu C-4 is 6% to 10% (Fig. 3). Assuming this value represents the ^{13}C commitment to TCAP cyclicity, the isotopic pattern expected in Glu would be C-4, 15% (observed value), C-3, 2.6% (=[15 − 1.1] × 0.1 + 1.1), and C-2, 1.2% (=[2.6 − 1.1] × 0.1 + 1.1). We obtained here larger ^{13}C-enrichment values (4.5% and 2.5% in C-3 and C-2, respectively), suggesting other pathways fed the TCAP with ^{13}C. We therefore believe that the contribution of TCAP cyclicity to ^{13}C patterns found here was of little importance under our conditions.

The involvement of the conversion of pyruvate back to PEP further agrees with the {^{13}C-^{13}C} interactions between atom positions in Glu. Although slight (near 4% ^{13}C), labeling in Glu C-3 was associated with that in C-4 and C-2 (62% interaction), showing the concerted input of ^{13}C-oxaloacetate (formed from ^{13}C-PEP) and ^{13}C-acetyl-CoA upon ^{13}C-3-pyruvate feeding (Figs. 1 and 3).

When fed with *d*-^{13}C-3-pyruvate, the deuterium content in Glu C-4 is lower (34%) than that in source pyruvate (50%). Since there was no hydrogen/deuterium isotope effect associated with the ^{13}C-commitment rate under our conditions, such a loss of deuterium likely came from the isotopic wash out to the solvent caused by the keto-enol equilibrium of pyruvate. The spontaneous equilibrium in water disfavors strongly the enol form (K_{eq} 2 × 10^{-5}; Esposito et al., 1999), with a very low rate constant of keto-to-enol conversion (around 10^{-6} s^{-1}). Such a value would give, in our 3-h experiment, an estimated proton exchange with the solvent of 10^{-6} s^{-1} × 15 × 10^{-3} mol L^{-1} × 3 × 3,600 = 0.16 mmol L^{-1} experiment^{-1} that is, 1% only of source pyruvate concentration. In other words, most of the deuterium loss in Glu C-4 was due to metabolic (enzymatic) effects, demonstrating that ^{13}C-3-pyruvate molecules underwent enolization, likely back to PEP. This process was nevertheless a dynamic equilibrium that reformed pyruvate so that Glu C-4 was only partially deuterated.

The metabolic flux associated with the conversion of pyruvate back to PEP may be roughly estimated with the ^{13}C-enrichment pattern in Glu C-4 and C-2 (Fig. 1). The ^{13}C-percentage excess (compared to natural abundance) in C-4 was nearly 15 − 1.1 approximately 14% and that in C-2 was 3 − 1.1 approximately 2%. Neglecting multiple rounds of the TCAP cycle, the relative commitment of pyruvate to PEP and oxaloacetate was then 2/14 = 14% of the commitment of

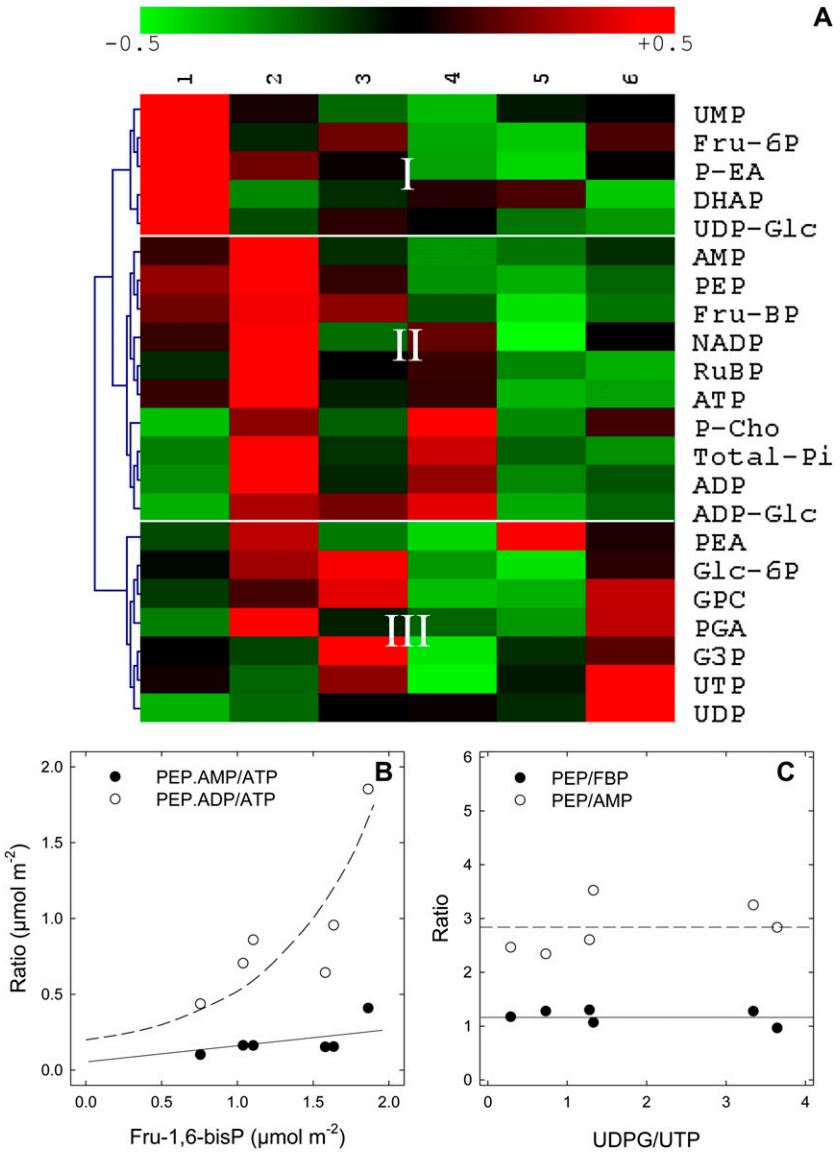

Figure 6. Natural variations in phosphometabolite content in illuminated cocklebur leaves, under 400 μmol mol^{-1} CO_2, 21% O_2, 23.5°C, 300 μmol mol^{-1} PAR, fed with pyruvate through the transpiration stream. A, Array representation of the phosphometabolome. Metabolites were quantified by liquid chromatography/time-of-flight mass spectrometry (ATP, ADP, AMP, UDP-Glc, ADP-Glc, UTP, UDP) and ^{31}P-NMR (others). The hierarchical clustering (left) was carried out with the cosine correlation on mean-centered metabolite contents. The range of the natural variation of phosphometabolites is ±50% (color scale on top). Column numbers on top (1–6) are biological replicates. DHAP, Dihydroxyacetone phosphate; G3P, glyceraldehyde-3-phosphate; GPC, glyceryl-phosphophorylcholine; P-Cho, phosphorylcholine; PEA, phosphatidyl-ethanolamine; P-EA, 3-phosphoryl-ethanolamine; PGA, phosphoglycerate; RuBP, ribulose-1,5-bisphosphate. B, Mass action ratio of phosphometabolites on the pyruvate kinase (PEP.ADP/ATP, white symbols) and PPDK (PEP.AMP/ATP, black symbols) as a function of Fru-1,6-bisphosphate. C, PEP content relative to Fru-1,6-bisphosphate (black symbols) or AMP (white symbols) as a function of UDP-Glc-UTP ratio, an indicator of Suc synthesis. In both B and C, metabolite concentrations are given in μmol m^{-2}. Continuous and dashed lines represent the apparent trends of the curves.

pyruvate to the TCAP via acetyl-CoA. Tcherkez et al. (2008) estimated that under similar conditions (pyruvate feeding in the light), the pyruvate-decarboxylating TCAP activity is 0.02 μmol m^{-2} s^{-1} and so the flux associated with conversion back to PEP would be near 0.002 μmol m^{-2} s^{-1}. In intact illuminated leaves, assuming a day respiration rate of 0.5 μmol m^{-2} s^{-1} and a natural TCAP activity of around 0.05 μmol m^{-2} s^{-1} (near 10% of the day CO_2 evolution rate), PEP resynthesis would be of 0.005 μmol m^{-2} s^{-1} (say, roughly 0.5‰ only of the net assimilation rate).

Which Is the Enzyme of PEP/Pyruvate Metabolism?

PEP resynthesis from pyruvate may involve pyruvate kinase or PPDK. Pyruvate kinase has been shown to be reversible, with a huge equilibrium constant of $10^{11.5}$ toward pyruvate production (nearly irreversible; Nageswara-Rao et al., 1979; Supplemental Table S1). Still, proton exchange between pyruvate and solvent water has been demonstrated (Robinson and Rose, 1972; Rose et al., 1991), showing the ability of the enzyme to catalyze the reverse reaction. However, the mass action ratio [pyruvate × ADP]/[PEP × ATP] is less favorable in the light than in the dark, with a larger leaf ATP-ADP ratio in the light (Fig. 5). Subcellular analysis of barley (*Hordeum vulgare*) protoplasts also showed that the ATP-ADP ratio was larger in both the chloroplast and cytosol in the light (Gardeström, 1987, but see Stitt et al., 1982), thereby disfavoring the pyruvate kinase activity, which is inhibited by ATP (Baysdorfer and Bassham, 1984). In vitro studies have further shown that major compounds such as Glu inhibit cytosolic pyruvate kinase and photosynthetic intermediates inhibit chloroplastic pyruvate kinase (Lin et al., 1989). It is therefore believed that both

chloroplastic and cytosolic pyruvate kinase activity is down-regulated in illuminated leaves (Plaxton, 1996).

By contrast, chloroplastic PPDK is activated in the light due to its reversible dephosphorylation by Pi, which is in turn converted to PPi (Chastain et al., 2002; Chastain and Chollet, 2003). The inactivation of the enzyme involves phosphorylation by ADP, converted to AMP. Therefore, both Pi-PPi and ADP-AMP ratios may be of importance to control PPDK (de)phosphorylation. Furthermore, such ratios have a thermodynamic effect on the reaction catalyzed by PPDK, the K_{eq} of which is around 100 only (Supplemental Table S1). That is, the reaction is much more reversible than pyruvate kinase. We found an ADP-AMP ratio of 1.3 and 2.3 in the light and in the dark, respectively (Fig. 5). In illuminated isolated chloroplasts, a low ADP-AMP ratio was observed, whereas the Pi concentration was quite high (up to 25 mmol L^{-1}; Santarius and Heber, 1965) and PPi concentration was believed to be very low (Edwards et al., 1978). It is thus likely that both the dephosphorylation of PPDK and the PEP-forming reaction of the equilibrium are promoted by light in chloroplasts. In the cytosol, Pi concentration is certainly lower, less than 1 millimolar (Bligny et al., 1990) and more probably near 70 μmol L^{-1} (Pratt et al., 2009). By contrast, PPi is predominantly in the cytosol, up to 0.3 mmol L^{-1} (Weiner et al., 1987), possibly due to the absence of cytosolic inorganic pyrophosphatase (Farré et al., 2006, but see Rojas-Beltrán et al., 1999). Furthermore, the cytosolic ATP-AMP ratio is similar (7–8) in the light and in the dark (Stitt et al., 1982). The PPDK-catalyzed reaction is thus slightly less favorable in the cytosol than in the chloroplast under illumination, but may still be driven by the very large ATP-AMP ratio.

We thus hypothesize here that the conversion of pyruvate back to PEP involves PPDK rather than pyruvate kinase. Accordingly, our results indicate that the leaf PPDK activity in the light is larger than in the dark (Fig. 5), as already shown elsewhere (Chastain and Chollet, 2003).

Rationale of PEP Resynthesis from Pyruvate

Leaf PPDK activity is influenced by light/dark conditions (see just above) and therefore, the biological significance of the PPDK flux is certainly related to the control of day respiration and pyruvate metabolism. We nevertheless recognize that at the leaf level, PPDK activity is believed to be heterogenous, with larger values in vein tissues (Hibberd and Quick, 2002). It is therefore possible that the PPDK activity observed here was partly associated with vascular cells, which require PEP for lignin biosynthesis. However, the labeling in major metabolites associated with PEPc-catalyzed C fixation (malate) or nitrogen fixation (Glu) was very clear (Fig. 2), suggesting a wider implication of the PPDK flux in cocklebur leaves. In fact, PEP resynthesis by the PPDK has been assumed to be involved in nitrogen assimilation. First, in senescing Arabidopsis leaves, the conversion of pyruvate back to PEP sustains oxaloacetate synthesis via the PEPc, thereby promoting Gln production for nitrogen remobilization (Taylor et al., 2010). Second, transcripts encoding PPDK have been reported to be more abundant in roots of rice (*Oryza sativa*) lines overexpressing Ala aminotransferase (AlaAT) as compared to the wild type (Beatty et al., 2009). Since AlaAT promotes nitrogen uptake and subsequent metabolism by the downstream catalysis of Ala to pyruvate (with the concomitant usage of 2-oxoglutarate and the formation of Glu), this suggests a role of PPDK in the recovery of oxaloacetate for Glu production.

In illuminated leaves, the PPDK activity may have further roles. As stated above, cytoplasmic pyruvate consumption is believed to be lower in the light compared to the dark, due to the partial inhibition of the PDH and the substantial inhibition of the TCAP. It is therefore plausible that PEP resynthesis contributes to preventing from pyruvate overaccumulation. In addition, PEP may be exchanged between the chloroplast and the cytoplasm (exchanged against Pi) through specific transporters (PPT1 and PPT2 in Arabidopsis; for review, see Linka and Weber, 2010). In the chloroplast, PEP is a fundamental precursor of aromatic amino acids and fatty acids (via pyruvate) and activates ADP-Glc synthesis (Ghosh and Preiss, 1966). Pyruvate (with glyceraldehyde-3-P) is also the precursor of methylerythritol, a key intermediate of chloroplastic isoprenoid synthesis (Rohmer et al., 1993, 1996). Isoprenoid production is believed to be substantial in illuminated leaves at moderate to high temperature, with the accumulation of 2-*C*-methyl-D-erythritol 2,4-cyclodiphosphate, which may in turn sequestrate most of stromal phosphate (Rivasseau et al., 2009). Therefore, sustaining the chloroplast with PEP molecules of cytosolic origin might be beneficial to maintain stromal pyruvate and Pi contents.

The PPDK consumes Pi and synthesizes PPi, thereby affecting the phospho balance of the cell. Typically, the cytoplasmic PPDK-catalyzed reaction may contribute to maintaining a low cytoplasmic Pi content, for which homeostatic regulation appears critical (Rebeillé et al., 1983; Pratt et al., 2009) and/or PPi synthesis as an energy donor (Weiner et al., 1987; Dancer et al., 1990) at the expense of ATP.

In other words, conversion of pyruvate back to PEP likely play multiple roles upon illumination to: (1) promote PEP resynthesis for PEPc-catalyzed oxaloacetate synthesis associated with nitrogen assimilation or chloroplastic isoprenoid metabolism and (2) impede possible increase in cytoplasmic ATP-Pi ratio (e.g. under large photorespiratory conditions that generates substantial reducing equivalents in the mitochondrion). In fact, the PEP content appeared tightly correlated to ATP or photosynthetic phosphorylated metabolites and furthermore, the apparent mass action ratio of pyruvate kinase seemed to increase with Fru-1,6-bisphosphate content (Fig. 5). PEP resynthesis from pyruvate might thus be involved in catabolic versus photosynthetic adjustments. We nevertheless

recognize that the control exerted by pyruvate-to-PEP conversion on the whole respiratory pathway is probably minor since the associated flux is rather small under our experimental conditions. Further work is needed (e.g. characterizing PPDK mutants) to identify which one of the metabolic roles mentioned above is the most significant.

MATERIALS AND METHODS

Plant Material and Gas Exchange

Growth conditions of cocklebur (*Xanthium strumarium*) plants and gas-exchange techniques were already described in Tcherkez et al. (2009). The third or fourth leaf (from the apical bud) was used for all measurements. Detached leaves were placed in a large gas-exchange cuvette connected to the open system Li-Cor 6400. In all experiments, photosynthesis was allowed to stabilize before labeling and then leaves were labeled for 3 h ($^{13}CO_2$ and/or ^{13}C pyruvate). $^{13}CO_2$ (99% ^{13}C) and $^{12}CO_2$ were purchased at Eurisotop and Air Liquide, respectively. For NMR analyses, the leaf was instantly frozen at the end of the labeling period with a freeze-spray system: Liquid nitrogen was sprayed instantly, that is, 0.1 s after the puncture of the upper wall of the chamber. The leaf sample was then kept at −80°C.

NMR Analyses

NMR measurements were carried out as described in Tcherkez et al. (2005) from perchloric acid extracts prepared from approximately 7 g of frozen leaf material. Spectra were obtained using a Bruker spectrometer (AMX 400, Bruker) equipped with a 10-mm multinuclear probe tuned at 100.6 (^{13}C) and 161.9 MHz (^{31}P). The assignment of ^{13}C and ^{31}P resonance peaks was carried out according to Gout et al. (1993) and Bligny et al. (1990), respectively. Peak intensities were normalized to a known amount of the internal reference compound (maleate for ^{13}C and methyl-phosphonate for ^{31}P) that was added to the sample (internal standard). Two types of control were done for NMR analyses: experiments with water (no labeling substrates) and those with ^{12}C substrates. The latter control was required to normalize the ^{13}C signal after ^{13}C labeling so as to calculate the ^{13}C percentage (% ^{13}C).

Liquid-Chromatography Time-of-Flight Mass Spectrometry

A 500-μL aliquot of the perchloric extract (see above, "NMR Analyses") was preleved and stored at −80°C for further use. Ten microliters of phosphoric acid (50%) were added to the extract and then a double solid phase extraction was carried out, using Strata-X-C and Strata-A-W columns (Phenomenex). Eluates were speed-vac dried and resuspended in water. Samples were injected in the UPLC Acquity equipped with the column UPLC-HSS T3 (2.1 × 100 mm, 1.8 μm; Waters) under an ammonium acetate/methanol gradient (99/1-0/100%, 6 min). Electrospray mass spectrometry was carried out with the MicrOTOF II (Bruker Daltonics) with N_2 (spray gas) upon negative ionization. All compounds analyzed here were measured against a calibration curve with pure standards purchased at Sigma-Aldrich.

PPDK Activity

The procedure used to determine PPDK leaf activity was inspired from Aoyagi and Bassham (1983) and Nakamoto and Edwards (1983). About 1 g of leaf frozen material was ground at 4°C using a cold mortar and 1 mL extracting buffer (0.1 M Tris-HCl, pH 7.5, 10 mM $MgCl_2$, 5 mM sodium pyruvate, 2 mM K_2HPO_4, 1 mM EDTA, 1% w/v sodium ascorbate, 10 mM β-mercaptoethanol, 1% w/v polyvinylpyrrolidone). The homogenate was filtered through one layer of nylon mesh (30-μm pore size), then briefly centrifugated (1 min at 990 rpm) and desalted with a NAP-5 column (GE Healthcare) previously equilibrated with 0.1 M Tris-HCl, 10 mM $MgCl_2$, 1 mM EDTA, 1% w/v sodium ascorbate, 10 mM β-mercaptoethanol at pH 7.5. PPDK activity was assayed spectrophotometrically (PEPc-malate dehydrogenase coupled assay) as described previously (Edwards et al., 1980).

Chemicals

Chemicals for assays and isotopic products, ^{13}C-3-pyruvate (99% ^{13}C in C-3) and *d*-^{13}C-3-pyruvate (50% D and 99% ^{13}C in C-3), were purchased at Isotec Sigma-Aldrich. *d*-^{12}C-pyruvate (50% D; used as an isotopic control for labeling experiments) was synthesized from natural pyruvate incubated for 48 h in deuterium oxide (D_2O) at 21°C, after Long and George (1960). In all cases, the final pyruvate concentration used in the experiments was 0.015 mol L^{-1}. The solutions were fed to leaves through the transpiration stream. *d*-^{13}C-3-pyruvate solutions used in experiments were prepared just before the onset of labeling, to minimize the spontaneous keto-enol equilibrium of pyruvate.

Supplemental Data

The following materials are available in the online version of this article.

Supplemental Figure S1. NMR signal of C-2 and C-4 atoms in 2-oxoglutarate.

Supplemental Table S1. Thermodynamic properties of pyruvate kinase and PPDK.

Received May 25, 2011; accepted June 30, 2011; published July 5, 2011.

LITERATURE CITED

Aoyagi K, Bassham JA (1983) Pyruvate orthophosphate dikinase in wheat leaves. Plant Physiol **73:** 853–854

Atkin OK, Millar AH, Gärdestrom P, Day DA (2000) Photosynthesis, carbohydrate metabolism and respiration in leaves of higher plants. *In* RC Leegood, TD Sharkey, S von Caemmerer, eds, Photosynthesis, Physiology and Metabolism. Kluwer Academic Publisher, London, pp 203–220

Baysdorfer C, Bassham JA (1984) Spinach pyruvate kinase isoforms: partial purification and regulatory properties. Plant Physiol **74:** 374–379

Beatty PH, Shrawat AK, Carroll RT, Zhu T, Good AG (2009) Transcriptome analysis of nitrogen-efficient rice over-expressing alanine aminotransferase. Plant Biotechnol J **7:** 562–576

Bligny R, Gardeström P, Roby C, Douce R (1990) ^{31}P NMR studies of spinach leaves and their chloroplasts. J Biol Chem **265:** 1319–1326

Budde RJA, Randall DD (1990) Pea leaf mitochondrial PDH complex is inactivated in vivo in a light-dependent manner. Proc Natl Acad Sci USA **87:** 673–676

Chastain CJ, Chollet R (2003) Regulation of pyruvate orthophosphate dikinase by ADP/Pi dependent reversible phosphorylation in C_3 and C_4 plants. Plant Physiol Biochem **41:** 523–532

Chastain CJ, Fries JP, Vogel JA, Randklev CL, Vossen AP, Dittmer SK, Watkins EE, Fiedler LJ, Wacker SA, Meinhover KC, et al (2002) Pyruvate, orthophosphate dikinase in leaves and chloroplasts of C_3 plants undergoes light-/dark-induced reversible phosphorylation. Plant Physiol **128:** 1368–1378

Dancer J, Veith R, Feil R, Komor E, Stitt M (1990) Independent changes of inorganic phyrophosphate and the ATP/ADP or UTP/UDP ratios in plant cell suspension cultures. Plant Sci **66:** 59–63

Doubnerová V, Ryšlavá H (2011) What can enzymes of C photosynthesis do for C plants under stress? Plant Sci **180:** 575–583

Dyson RD, Cardenas JM, Barsotti RJ (1975) The reversibility of skeletal muscle pyruvate kinase and an assessment of its capacity to support glyconeogenesis. J Biol Chem **250:** 3316–3321

Edwards GE, Robinson SP, Tyler NJC, Walker DA (1978) Photosynthesis by isolated protoplasts, protoplast extracts, and chloroplasts of wheat: influence of orthophosphate, pyrophosphate, and adenylates. Plant Physiol **62:** 313–319

Edwards GE, Ujihira M, Sugiyama T (1980) Light and temperature dependence of the rate and degree of activation of pyruvate, Pi dikinase *in vivo* in maize. Photosynth Res **1:** 199–207

Esposito A, Lukas A, Meany JE, Pocker Y (1999) The reversible enolization and hydration of pyruvate: possible roles of keto, enol, and hydrated pyruvate in lactate dehydrogenase catalysis. Can J Chem **77:** 1108–1117

Farré EM, Tech S, Trethewey RN, Fernie AR, Willmitzer L (2006) Subcellular pyrophosphate metabolism in developing tubers of potato (*Solanum tuberosum*). Plant Mol Biol **62:** 165–179

Gardeström P (1987) Adenylate ratios in the cytosol, chloroplasts and

mitochondria of barley leaf protoplasts during photosynthesis at different carbon dioxide concentrations. FEBS Lett **212:** 114–118

Gauthier PP, Bligny R, Gout E, Mahé A, Nogués S, Hodges M, Tcherkez GG (2010) In folio isotopic tracing demonstrates that nitrogen assimilation into glutamate is mostly independent from current CO_2 assimilation in illuminated leaves of *Brassica napus*. New Phytol **185:** 988–999

Ghosh HP, Preiss J (1966) Adenosine diphosphate glucose pyrophosphorylase: a regulatory enzyme in the biosynthesis of starch in spinach leaf chloroplasts. J Biol Chem **241:** 4491–4504

Gout E, Bligny R, Pascal N, Douce R (1993) The C-13 nuclear magnetic resonance studies of malate and citrate synthesis and compartmentation in higher plant cells. J Biol Chem **286:** 3986–3992

Hanning I, Heldt HW (1993) On the function of mitochondrial metabolism during photosynthesis in spinach (*Spinacia oleracea* L.) leaves (partitioning between respiration and export of redox equivalents and precursors for nitrate assimilation products). Plant Physiol **103:** 1147–1154

Harding RW, Caroline DF, Wagner RP (1970) The pyruvate dehydrogenase complex from the mitochondrial fraction of *Neurospora crassa*. Arch Biochem Biophys **138:** 653–661

Hibberd JM, Quick WP (2002) Characteristics of C_4 photosynthesis in stems and petioles of C_3 flowering plants. Nature **415:** 451–454

Kang HG, Park S, Matsuoka M, An G (2005) White-core endosperm floury endosperm-4 in rice is generated by knockout mutations in the C-type pyruvate orthophosphate dikinase gene (OsPPDKB). Plant J **42:** 901–911

Kok B (1948) A critical consideration of the quantum yield of *Chlorella* photosynthesis. Enzymologia **13:** 1–56

Krimsky I (1959) Phosphorylation of pyruvate by the pyruvate kinase reaction and reversal of glycolysis in a reconstructed system. J Biol Chem **234:** 232–236

Lasanthi-Kudahettige R, Magneschi L, Loreti E, Gonzali S, Licausi F, Novi G, Beretta O, Vitulli F, Alpi A, Perata P (2007) Transcript profiling of the anoxic rice coleoptile. Plant Physiol **144:** 218–231

Lin JF, Wu SH (2004) Molecular events in senescing *Arabidopsis* leaves. Plant J **39:** 612–628

Lin M, Turpin DH, Plaxton WC (1989) Pyruvate kinase isozymes from the green alga, Selenastrum minutum. II. Kinetic and regulatory properties. Arch Biochem Biophys **269:** 228–238

Linka N, Weber APM (2010) Intracellular metabolite transporters in plants. Mol Plant **3:** 21–53

Long DA, George WO (1960) Spectroscopic study of the pyruvate ion. Trans Faraday Soc **56:** 1570–1581

Marillia EF, Micallef BJ, Micallef M, Weninger A, Pedersen KK, Zou J, Taylor DC (2003) Biochemical and physiological studies of *Arabidopsis thaliana* transgenic lines with repressed expression of the mitochondrial pyruvate dehydrogenase kinase. J Exp Bot **54:** 259–270

McQuate JT, Utter MF (1959) Equilibrium and kinetic studies of the pyruvic kinase reaction. J Biol Chem **234:** 2151–2157

Nageswara Rao BD, Kayne FJ, Cohn M (1979) ^{31}P NMR studies of enzyme-bound substrates of rabbit muscle pyruvate kinase: equilibrium constants, exchange rates, and NMR parameters. J Biol Chem **254:** 2689–2696

Nakamoto H, Edwards GE (1983) Influence of oxygen and temperature on the dark inactivation of pyruvate orthophosphate dikinase and NADP-malate dehydrogenase in maize. Plant Physiol **71:** 568–573

Nunes-Nesi A, Sweetlove LJ, Fernie AR (2007) Operation and function of the tricarboxylic acid cycle in the illuminated leaf. Physiol Plant **129:** 45–56

Ohlrogge JB, Jaworski JG (1997) Regulation of fatty acid synthesis. Annu Rev Plant Physiol Plant Mol Biol **48:** 109–136

Paul MJ, Pellny TK (2003) Carbon metabolite feedback regulation of leaf photosynthesis and development. J Exp Bot **54:** 539–547

Plaxton WC (1996) The organization and regulation of plant glycolysis. Annu Rev Plant Physiol Plant Mol Biol **47:** 185–214

Pratt J, Boisson AM, Gout E, Bligny R, Douce R, Aubert S (2009) Phosphate (Pi) starvation effect on the cytosolic Pi concentration and Pi exchanges across the tonoplast in plant cells: an in vivo 31P-nuclear magnetic resonance study using methylphosphonate as a Pi analog. Plant Physiol **151:** 1646–1657

Rapp BJ, Miernyk JA, Randall DD (1987) Pyruvate dehydrogenase complexes from *Ricinus communis* endosperm. J Plant Physiol **127:** 293–306

Rebeillé F, Bligny R, Martin JB, Douce R (1983) Relationship between the cytoplasm and the vacuole phosphate pool in *Acer pseudoplatanus* cells. Arch Biochem Biophys **225:** 143–148

Rivasseau C, Seemann M, Boisson AM, Streb P, Gout E, Douce R, Rohmer M, Bligny R (2009) Accumulation of 2-*C*-methyl-D-erythritol 2,4-cyclodiphosphate in illuminated plant leaves at supraoptimal temperatures reveals a bottleneck of the prokaryotic methylerythritol 4-phosphate pathway of isoprenoid biosynthesis. Plant Cell Environ **32:** 82–92

Robinson JL, Rose IA (1972) The proton transfer reactions of muscle pyruvate kinase. J Biol Chem **247:** 1096–1105

Rohmer M, Knani M, Simonin P, Sutter B, Sahm H (1993) Isoprenoid biosynthesis in bacteria: a novel pathway for the early steps leading to isopentenyl diphosphate. Biochem J **295:** 517–524

Rohmer M, Seemann M, Horbach S, Bringer-Meyer S, Sahm H (1996) Glyceraldehyde 3-phosphate and pyruvate as precursors of isoprenic units in an alternative non-mevalonate pathway for terpenoid biosynthesis. J Am Chem Soc **118:** 2564–2566

Rojas-Beltrán JA, Dubois F, Mortiaux F, Portetelle D, Gebhardt C, Sangwan RS, du Jardin P (1999) Identification of cytosolic Mg^{2+}-dependent soluble inorganic pyrophosphatases in potato and phylogenetic analysis. Plant Mol Biol **39:** 449–461

Rose IA, Kuo DJ, Warms JVB (1991) A rate-determining proton relay in the pyruvate kinase reaction. Biochemistry **30:** 722–726

Santarius KA, Heber U (1965) Changes in the intracellular levels of ATP, ADP, AMP and P1 and regulatory function of the adenylate system in leaf cells during photosynthesis. Biochim Biophys Acta **102:** 39–54

Scheible WR, Krapp A, Stitt M (2000) Reciprocal diurnal changes of PEPc expression, cytosolic pyruvate kinase, citrate synthase and NADP-isocitrate dehydrogenase expression regulate organic acid metabolism during nitrate assimilation in tobacco leaves. Plant Cell Environ **23:** 1155–1167

Stitt M, Lilley RM, Heldt HW (1982) Adenine nucleotide levels in the cytosol, chloroplasts, and mitochondria of wheat leaf protoplasts. Plant Physiol **70:** 971–977

Taylor L, Nunes-Nesi A, Parsley K, Leiss A, Leach G, Coates S, Wingler A, Fernie AR, Hibberd JM (2010) Cytosolic pyruvate,orthophosphate dikinase functions in nitrogen remobilization during leaf senescence and limits individual seed growth and nitrogen content. Plant J **62:** 641–652

Tcherkez G, Bligny R, Gout E, Mahé A, Hodges M, Cornic G (2008) Respiratory metabolism of illuminated leaves depends on CO_2 and O_2 conditions. Proc Natl Acad Sci USA **105:** 797–802

Tcherkez G, Cornic G, Bligny R, Gout E, Ghashghaie J (2005) In vivo respiratory metabolism of illuminated leaves. Plant Physiol **138:** 1596–1606

Tcherkez G, Mahé A, Gauthier P, Mauve C, Gout E, Bligny R, Cornic G, Hodges M (2009) In folio respiratory fluxomics revealed by ^{13}C isotopic labeling and H/D isotope effects highlight the noncyclic nature of the tricarboxylic acid "cycle" in illuminated leaves. Plant Physiol **151:** 620–630

Tovar-Méndez A, Miernyk JA, Randall DD (2003) Regulation of pyruvate dehydrogenase complex activity in plant cells. Eur J Biochem **270:** 1043–1049

Weiner H, Stitt M, Heldt HW (1987) Subcellular compartmentation of pyrophosphate and alkaline pyrophosphatase in leaves. Biochim Biophys Acta **893:** 13–21